MULTI-EPOCH INTERFEROMETRIC STUDY OF MIRA VARIABLES I. Narrowband diameters of RZ Peg and S Lac

R. R. Thompson[1,2]

M. J. Creech-Eakman[1,3]

and

G. T. van Belle[1]

Received _____; accepted _____

[1]Jet Propulsion Laboratory, California Institute of Technology, MS 171-113, 4800 Oak Grove Drive, Pasadena CA 91109-8099. (thompson@huey.jpl.nasa.gov)

[2]University of Wyoming, Dept of Physics and Astronomy, PO Box 3905, Laramie WY 82071-3905

[3]California Institute of Technology/JPL Post-doctoral Scholar.

ABSTRACT

As part of the long-term monitoring of Mira variables at the Palomar Testbed Interferometer, we report high-resolution narrowband angular sizes of the oxygen-rich Mira S Lac and the carbon-rich Mira RZ Peg in the near-infrared. The dataset spans three pulsation cycles for S Lac and two pulsation cycles for RZ Peg (a total of 1070 25-sec observations), and represents the first study to correlate multi-epoch narrowband interferometric data of Mira variables. When the calibrated visibility data are fit using a uniform disk brightness model, differences are seen in their angular diameters as a function of wavelength within the K band (2.0 - 2.4 μm); the source of which is believed to be molecular absorptions in or above the photospheres of the two chemically different Miras. Using visible photometric data provided by the AFOEV, the continuum minimum size of RZ Peg lags this by 0.28 $\pm$ 0.02 in pulsation, similar to the phase lag found in CORAVEL radial velocity data. However, for S Lac, the continuum minimum size tracks the visual maximum brightness. Based on the mean of the continuum angular diameter cycloids, basic stellar parameters are computed for both RZ Peg and S Lac, with both showing maximum atmospheric extension with respect to the 2.0 and 2.4 μm diameters near phase 0.9. Using the mean value of the fitted cycloids, RZ Peg has a radius R_{mean} = 377 $\pm$ 111 $R_\odot$ and a mean T_{eff} = 2706 $\pm$ 36 K ; S Lac has a radius R_{mean} = 292 $\pm$ 73 $R_\odot$ and a mean T_{eff} = 2605 $\pm$ 47 K . The dominant source of error in the radii is the large uncertainty in the distances to these two stars.

Subject headings: technique: interferometric—stars: AGB and post-AGB—stars: late-type—stars: fundamental parameters—stars: atmospheres—stars: individual (RZ Peg, S Lac) —infrared: stars—stars: variable—stars: late-type

1. Introduction

Mira variable stars are classified as long-period variables (LPV) with periods from 150 to 500 d, and are lumiosity class III giants. As a result of stellar pulsations, atmospheric shocks are set up which extend the outer atmospheres of these variable stars, as well as provide a mechanism for mass loss. Interferometric measurements of Mira variables provide information on such derived parameters as linear radii and effective temperatures (T_{eff}). Wideband angular diameters have traditionally been employed to facilitate a better understanding of these parameters (van Belle et al. 1996, 1997; Perrin et al. 1999; Thompson, Creech-Eakman & Akeson, 2001; Creech-Eakman & Thompson, 2001.). While these studies provide important insights into the gross physical properties of Mira variables, the nature of the wideband measurements do not lend themselves to exploring angular size changes with respect to the chemical composition of these enigmatic stars.

Comparisons between continuum and molecular line bands in narrowband visibility data give insight into the spatial extent of the molecular-forming regions around these types of stars. A number of studies have recently been conducted in which narrowband visibility data have been collected in these continuuum and molecular line bands. Cyclic variations both in and out of the TiO molecular band (905 nm) were reported by Young et al. (2000) for the Mira χ Cyg using the Cambridge Optical Aperature Synthesis Telescope (COAST, Baldwin et al. 1994). Size changes of 45% in amplitude (with respect to the minimum size) were detected in the TiO band, while J-band (1.25 μm) observations suggested little or no such size changes. The interpretation given was the different photospheric layers (or combination of layers) were seen in the two bands. The higher, cooler layers where the TiO molecules are formed vary in opacity with pulsation phase (Spinrad & Wing 1969), and enlarges the apparent size of the star within the TiO band. While size changes in the continuum bands are normally attributed to bulk motion of the stellar photosphere, size

changes in molecular bands are attributed to changes in opacity of those molecules.

Jacob et al. (2000) also used the TiO bands to explore the angular size of the oxygen-rich Mira R Dor using the Masked Aperture-Plane Interferometric Telescope (Bedding, Robertson & Marson 1994). Their study compares models with observed data, and finds that models tend to underestimate the observed variation of visibilities with wavelength. Using COAST, Burns et al. (1998) report angular size variations of R Leo with respect to pulsation phase in TiO bands (833 and 940 nm), and show that maximum size corresponds to visual minimum light with size variations were 35% (peak-to-peak) in amplitude. Visibility data at 11.15 μm taken with the Infrared Spatial Interferometer (ISI, Hale et al. 2000), when combined with narrowband near-infrared visibility data taken with the pupil-masking technique at the Keck Observatory, provided detailed spatial information for the star R Aqr (Tuthill et al. 2000). These multi-wavelength data on R Aqr do not support the current models of this symbiotic star.

While these studies provide important information as to the spatial extent of molecular species at visible wavelengths, narrowband visibility observations in the near-infrared are lacking. Narrowband visibility measurements in the near infrared can provide information on such molecular species as CO, H_2O, CN, and many others. Using the technique of high-resolution long baseline Michelson interferometry, we present narrowband observations in the K band of the oxygen-rich Mira S Lac and the carbon-rich Mira RZ Peg over multiple pulsation epochs. Quirrenbach (2001) stresses the importance and need for systematic observations of narrowband intererometric data on Mira variables covering a full pulsation cycle in order to test critically current models, which still cannot explain fully the atmospheres of these variable stars. The data presented here can be used as observational constraints on the oxygen-rich visibility models currently in the literature (Bessell, Scholz & Wood 1996; Hofmann, Scholz & Wood 1998).

2. Observations and Data Reduction

Observations were made in the K band using the Palomar Testbed Interferometer (PTI), as described by Colavita et al. (1999). The data were taken between 1999 and 2001 using the north-south baseline (110 m projected maximum), and represent a combined total of 1070 25-sec observations from 34 individual nights. The data were calibrated using a standard method as described by Boden et al. (1998). The wideband visibility data are synthesized using five spectrometer channels across the K band. The spectrometer channels span the wavelength range 2.0–2.4 μm, yielding an effective bandwidth of 0.097 μm and a resolution ($\lambda/\Delta\lambda$) of R $\simeq$ 23 with respect to the center channel at 2.2 μm. Details of the spectrometer channel visibility measurments, including readout, bias-correction and signal-to-noise, may be found elsewhere (Colavita 1999).

The system visibility was measured with respect to two calibration stars, with small angular sizes ($\simeq$0.8 mas) that are not strongly resolved by PTI; this minimizes any spectral dependence with angular size for the calibrators. The sizes of the calibrators were initially estimated using a blackbody fit to published photometric data. Calibrator sizes were iterated until a consistent solution converged with respect to the target-calibrator pairs for the observations. In this way, the angular diameters of the target and the two calibrators are self-consistent. The solution for the calibrator diameters were then used for all subsequent calibrations in both wideband and narrowband data (Table 1). The adopted sizes of the primary calibrator stars based on observation are slightly smaller than their bolometric estimates. However, the differences are within the 15% error bars in size ($\simeq$ 0.1 mas) that we have adopted for the observational sizes, Two stars were used to calibrate RZ Peg and S Lac, selected for proximity to the targets. Error bars on the calibrated visibilities of both RZ Peg and S Lac represent a combination of the scatter between the two target-calibrator measurements and the internal scatter of the visibilities. Both calibrator sizes were checked

for internal consistency on the nights the data were taken, and show no significant change in apparent angular size within the stated uncertainties.

All apparent angular diameters were fit to the visibility data using a uniform disk brightness model (UD), in both the synthetic wideband channel and the five narrowband channels. The predicted visibility for the uniform disk model is a function of the projected baseline (B), wavelength of observation (λ), and apparent angular size (θ) such that

$$V^2 = \left(2\frac{J_1(\pi\theta B/\lambda)}{(\pi\theta B/\lambda)}\right)^2 \quad (1)$$

where J_1 is the first-order Bessel function. For all UD angular sizes, a conservative approach was taken such that a lower error limit of 0.02 mas was assigned if the calculated uncertainty was smaller than this value. This limit represents an uncertainty of 0.5 % in squared visibility for the near-infrared at 100 m in the diameter range of the targets (2.5 – 3.5 mas).

3. Results

The representative spectral angular diameters of the Miras RZ Peg and S Lac are plotted in Fig. 1. For each Mira, the spectral angular diameter of a non-Mira of similar chemical class is also plotted for comparison. These diameters are the mean of the data from one night of observation; spherical symmetry is assumed (a much more rigorous analysis for departures from spherical symmetry will be forthcoming in another paper). For the oxygen-rich Mira S Lac, a definite minimum size is seen at the band center (2.2 μm). This shape is also seen in o Cet in the K-band by Tuthill, Monnier & Danchi (1999) using the pupil-masking technique at the Keck telescope. The spectral dependence of the angular diameter for S Lac (i.e. the 2.0 μm size being slightly smaller than the 2.4 μm size) typifies what is seen in the PTI Mira database for Mira stars of mid-M class. Those

of earlier M class tend to have a more symmetric spectral trace, while those of late M-class have 2.0 μm sizes only slightly larger than the 2.2 μm size (Thompson 2002). As compared to a non-Mira of similar chemical composition, the spectral shape of the M2 III non-Mira also depicts a similar “”V-shape” structure, but only barely statistically significant. When the 2.2 μm size is referenced to the band edges, the depth of this feature for oxygen-rich non-Miras is $\simeq$ 1%. For oxygen-rich Miras this depth is an order of magnitude higher (15 – 25%), presumably resulting from their extended atmospheric layers and/or abundance of opacity sources. With respect to the minimum sizes in each band for S Lac seen during the pulsation cycle, the peak-to-peak variations in angular size are 13, 22, and 12% for the bands 2.0, 2.2, and 2.4 μm, respectively.

As for the carbon-rich stars, the Mira RZ Peg displays a positive slope across the wavelength band with respect to angular size. Unlike the oxygen-rich S Lac, the 2.0 μm sizes are always smaller than the 2.2 μm (or “continuum”) size. Again, the spectral angular diameter shape of RZ Peg typifies that seen in the carbon-rich Miras of the PTI dataset (Thompson 2002). While the non-Mira carbon star HIP 92194 displays a similar UD spectral trend as in the Mira RZ Peg, its slope across the K band is much smaller. Quantitatively, RZ Peg has a slope $\Delta\theta/\Delta\lambda = 1.90$ mas/μm, while the non-Mira carbon star has a slope $\Delta\theta/\Delta\lambda = 0.78$ mas/μm. An investigation into the nature of these shapes is presented in Section 4.5. With respect to the minimum sizes in each band for RZ Peg seen during the pulsation cycle, the peak-to-peak variations in angular size are in 30, 22, and 18% for the bands 2.0, 2.2, and 2.4 μm, respectively. Note that while size variations in the continuum are equal in value of both RZ Peg and S Lac, RZ Peg displays larger variations at the bandedges.

The narrowband angular diamaters with respect to phase for both Mira stars are given in Fig. 2. While data on all five spectral channels has been collected and reduced, only

the center "continuum" channel and the two bandedge channels are plotted. Size changes in the 2.1 μm and 2.3 μm channels follow similar trends to their neighboring bandedge channels. Phase information was deduced from data supplied by the Association Francaise des Observateurs d'Etoiles Variables (AFOEV). Data for RZ Peg span the pulsation phases 0.1 – 1.9 (epoch JD 2451372), with a derived period of 422.4 d. Data for S Lac span 0.7 – 3.9 (epoch JD 2451249), with a derived period of 240.6 d. Phases greater than unity denote subsequent cycles, and are denoted by different symbols in Fig. 2 (see caption). The derived periods differ from the GCVS published values (Kholopov, et al. 1998) by $\leq 3\%$ when fit to a simple sinusoid. Fit parameters to all diameter cycloids given in Fig. 2 appear in Table 2. While we do not imply that the two Miras vary in size in a simple sinusoidal manner, the fits in Fig. 2 allow one to extract basic amplitudes, phase offsets, and mean angular sizes with respect to visual pulsation phase.

The angular size changes as a function of time in both stars raises the question of possible binary companions. No significant changes (at the 2% V^2 level) on a night-to-night basis were seen for either star, except in one instance for RZ Peg (see Section 4.5). Furthermore, as demonstrated by Boden et al. (1998a), PTI is largely insensitive to companions with $\Delta K > 4$; thus, for each Mira the companion would have to have a magnitude brighter than $K \simeq 7$ to affect the measured visibilities. For a companion to remain undetected at visual magnitudes (for both Miras minimum light has a $V = 13$ magnitude), but affect the V^2 for the interferometer would require a V-$K = 6$. Further evidence against binarity exists in the form of archival data. In the case of S Lac, data from the *International Ultraviolet Explorer* did not reveal the presence of any far-ultraviolet (1200 - 3000 Å) emission, which would be indicative of a possible white dwarf companion (Burleigh, Barstow & Fleming 1997). Additionally, Lu et al. (1987) did not detect any companion for S Lac between 35 and 1000 mas of separation. Finally, Udry et al. (1998) ruled out the possibility of a companion in a binary search around RZ Peg while using the

CORAVEL spectro-velocimeter (Baranne, Mayor & Poncet 1979). Thus, effects due to a binary companion are ruled out in both Miras and the nature of the angular size changes are attributed to intrinsic atmospheric pulsation.

4. Discussion

4.1. Basic Stellar Parameters

4.1.1. The Miras

Wavelength-dependent apparent diameters found in Miras based upon UD model assumptions must be interpreted with caution (Scholz, 2001). Compact stellar atmospheres lend themselves well to the UD model, such as that seen in the comparison M2 III star in Fig. 1 with apparent angular diameters unchanging across the band at the 1% level. In the case of S Lac, however, assigning the apparent angular diameters within each band to a "real" stellar photospheric size is problematic at best. A single-baseline interferometer will measure visibilities based on amplitude information, with the phase information unusable due to the lack of a phase reference. As such, visibilities taken with a single baseline are exclusively model-dependent in their interpretation, and *a priori* assumptions must be made to interpret the results.

One of the first problems in interpreting the narrowband angular diameters of S Lac is in establishing a "continuum" channel for the five K-band channels which will lead to a determination of the stellar photospheric diameter. As H_2O is one of the most abundant molecules in the atmospheres of oxygen-rich Miras, it is also the dominant absorber in the near-infrared, with broad absorption features centered at 1.4, 1.9 and 2.7 μm. The wings of these broad features tend to contaminate continuum radiation in Mira variables, especially in the K band (Lançon & Rocca-Volmerange, 1992). Given the five spectral channels of the

PTI data, the least affected by the opacity effects from H_2O would be the center channel at 2.2 μm. However, even visibility data from the 2.2 μm channel may still not fully represent the continuum size, and would tend to overestimate the size of the stellar photosphere. (The "stellar photosphere" is defined as the region of continuum-forming layers of the star.) Despite this effect for S Lac, the data in the 2.2 μm channel is adopted to represent the continuum in the K band.

The determination of a continuum size for the carbon-rich Mira RZ Peg is equally challenging. While H_2O is the dominant source of opacity in oxygen-rich Miras, CN is an important source of opacity in carbon stars. The K-band opacity effects due to CN were described by Wing & Spinrad (1970) as "moderate" as compared to opacity effects due to CO, thus making CN significant enough to warrant consideration. The $\Delta\nu$ = -2 transitions of the CN red system ($A^2\Pi$ - $X^2\Sigma$) appear as four bandheads within the K band, excluding molecular isotopes of this molecule, with each CN bandhead of this system existing within the first four PTI spectral channels. Additionally, HCN and C_2H_2 become a significant source of opacity in carbon giants, and can even overwhelm the CO opacity at low T_{eff} (Goebel et al. 1981). (The 2.4 μm channel is contaminated by the CO first overtone bandheads.) Despite the lack of a clean continuum channel in the case of carbon-rich Miras, we adopt the 2.2 μm channel as a continuum for RZ Peg in order to maintain consistency with the analyses of S Lac. Derived parameters for both Miras are given in Table 3; and, where angular-dependent quantities are calculated, the mean value of the best-fit 2.2 μm cycloid was used.

Miras which are enshrouded by molecular sources of opacity will appear cooler than their true photospheric temperatures. Using the mean angular diameter in the 2.2 μm channel, along with the bolometric flux derived from available photometry, results in T_{eff} $\simeq$ 2600 K for S Lac from the relation

$$T_{eff} = 2341 \left(\frac{F_{bol}}{\theta^2} \right)^{\frac{1}{4}} \quad (2)$$

with F_{bol} in units of erg/cm^2/sec and θ in mas. Following Lewis (1989), (25 - 12) μm and (60 - 25) μm *IRAS* colors were calculated (-0.84 and -1.25, respectively) and reveal that S Lac departs significantly from these same colors determined for a blackbody. This departure implies significant dust (or water ice, see Chiang et al. 2001) formation. However, given the low mass-loss rate of S Lac (section 4.2), this implies an event of high mass loss sometime in the past, whose source of opacity in the mid-infrared (dust or water ice) has had time to travel much farther out from the stellar photosphere to temperature regimes which do not affect the K band (Dyck et al. 1992). More significantly, Miras will appear larger and cooler than they actually are, as a result of dynamic atmospheric effects such as atmospheric extension and emission of post-shock cooling radiation (Beach, Willson & Bowen 1988). However, the relative changes in T_{eff} throughout the pulsation cycle based on the 2.2 μm angular size should offer a reasonable correlation with the true photospheric temperature changes. Based on the maximum and minimum sizes predicted by the 2.2 μm cycloid and a constant bolometric flux, the temperature variation due to pulsation is 250 K. This temperature amplitude is almost half of the value found for oxygen-rich Miras by van Belle et al. (1996) based on empirical angular diameters. The mean period of the resolved Miras by van Belle et al. (1996) is 372 d, and Whitelock (1986) has shown that larger mass loss is correlated to longer period and larger visual amplitude. Additionally, the source of H_2O opacity around S Lac may be masking the true temperature amplitude of the pulsating stellar photosphere. Additionally, the T_{eff} defined in Eq. (2) utilizes the 2.2 μm angular diameter, which may deviate from the effective temperature derived from the more standard 1.04 μm continuum wavelength or from the Rosseland mean opacity within our 2.2 $\pm$ 0.1 μm channel (cf. Bessell, Scholz & Wood, 1996; Hofmann, Scholz & Wood, 1998).

The determination of a continuum angular size for the carbon-rich RZ Peg is more straightforward than its oxygen-rich counterpart, owing to the lack of H_2O contamination within the K band for carbon-rich Miras. Using the available photometry to derive a bolometric flux in conjunction with the mean 2.2 μm angular diameter, a $T_{eff} \simeq 3100$ K is derived. This temperature is almost 500 K higher than the average found by van Belle et al. (1997) for carbon Miras. Knapik, Bergeat & Rutily (1999) classify RZ Peg as a CS star, and was given a "carbon variable index" typical of an unreddened carbon Mira (CVI) with $T_{eff} = 2800 - 2900$ K. Aoki, Tsuji & Ohnaka (1998) list RZ Peg as SC type and class it as C9.1e, using the scale of Yamashita (1972) for carbon stars. Of the five carbon Miras listed by van Belle et al. (1997), all of them were classified as CV6-CV7 by Bergeat, Knapik & Rutily (2001) (a follow-up study to the 1999 reference by the same authors). Thus, van Belle et al. (1997) chose carbon Miras with heavily reddened atmospheres, suggestive of dust-enshouded stars as a result of high mass loss. Conversely, RZ Peg as a CV1 is more "naked" a star than those studied by van Belle et al. (1997).

Following Lewis (1989) again for RZ Peg, (25 - 12) μm and (60 - 25) μm *IRAS* colors were calculated (-0.76 and -1.10, respectively) and reveal the carbon Mira has colors closer to a blackbody at these wavelengths than S Lac. Bergeat, Knapik & Rutily (2001) derive a $T_{eff} = 2852 \pm 37$ K for RZ Peg at phase 0.22, based on fitting a spectral energy distribution to photometric measurements at this phase. Using the model cycloid for the 2.2 μm diameter of RZ Peg, we derive $T_{eff} = 2594$ K at phase 0.22, which is lower than their derived temperature. Using the maximum and minimum sizes predicted by the 2.2 μm cycloid and a constant bolometric flux, the temperature variation due to pulsation is 270 K, and is comparable to that of the oxygen-rich S Lac for $(T_{max}\text{-}T_{min}) / T_{mean} = 0.1$.

4.1.2. The non-Mira Giants

For completeness, the sizes and T_{eff} of the non-Miras are given. Based upon available photometry in the literature for the M2 III star (HD 193347), we derive a bolometric flux of F_{bol} = 25.9 ± 1.9 x 10^{-8} erg/cm^2/s, and by Eq. (2), T_{eff} = 3782 ± 72 K. Based on the *Hipparcos* parallax of 3.96 ± 0.69 mas, the resulting linear size is 52.9 ± 9.5 $R_\odot$. This size is consistent with that determined by Dumm & Schild (1998) which utilized a *V-I* color index relation calibrated against published angular diameters of M-type giants, and is also consistent with their derived T_{eff} = 3820 K.

The carbon-rich non-Mira HIP 92914 (DR Ser; C6,II) is classified as a pulsating variable of type Lb. Available photometry exists in the literature (Gezari et al. 1999; Kerschbaum, Lazaro & Habison, 1996) to derive a bolometric flux F_{bol} = 17.6 ± 2.1 x 10^{-8} erg/cm^2/s. Using the 2.2 μm size in Fig. 1 results in a T_{eff} = 2578 ± 77 K, which is consistent with that derived by Bergeat, Knapik & Rutily (2001) of T_{eff} = 2650 K. The *Hipparcos* parallax is unusable, given a quoted value of 0.59 ± 1.48 mas. If the mean value of M_K = -6.84 ± 1.18 for Lb carbon stars is used (Wallerstein & Knapp, 1998) in conjunction with m_K=2.0 for HIP 92194, the corresponding distance range is 340 - 1000 pc. Converting the angular size of HIP 92194 to a linear radius results in a range of 125 - 370 $R_\odot$. While linear radii of C-type non-Mira stars based on empirical angular sizes do not as yet exist in the literature, the range of sizes for HIP 92194 is well in agreement with the results by van Belle & Thompson (1999) and van Belle et al. (2002), as well as in agreement with S-type non-Miras measured by van Belle et al. (1997).

4.2. Mass loss

To demonstrate that the opacity effects seen in the narrowband diameters of RZ Peg and S Lac are attributed to regions of opacity close to the stellar photospheres, we comment on the mass loss of each star. The mass-loss rates of RZ Peg for dust and gas, calculated by Groenewegen et al. (1998), are relatively low, with values 5 x 10^{-10} $M_{\odot}$/yr and 4.3 x 10^{-7} $M_{\odot}$/yr, respectively. While Lewis (1989) maintains that for oxygen-rich Miras, a visual amplitude of $\Delta m_V > 2.5$ signals the onset of mass loss, carbon Miras commonly can have lower visual amplitudes. Also, this magnitude change limit may be somewhat arbitrary (Wallerstein & Knapp, 1998). For RZ Peg, the best fit cycloid to the AFOEV visual data yield a $\Delta m_V = 4.8$. According to Jura (1986), carbon stars with periods $\geq$ 400 d show a trend of increasing mass loss with increasing $F_{\nu}(12\mu m)/F\nu(2\mu m)$ flux ratios. RZ Peg falls right at the beginning of this trend toward higher mass-loss, but the flux ratio places this star in an ambiguous region on the plot. As a result of this ambiguity and the large visual amplitude, it is unclear if RZ Peg is entering a transition from a low to a high mass-loss object.

The oxygen-rich S Lac also has a low rate of mass loss. Using colors extrapolated from the bolometric flux fit herein, the color relations by Le Bertre & Winters (1998) yield mass loss rates of 1 x 10^{-8} $M_{\odot}$/yr for *K-L'* and 0.7 x 10^{-8} $M_{\odot}$/yr for *J-K*. This is consistent with Bowen & Willson (1991) for a fundamental pulsator of large mass ($\simeq$ 2 $M_{\odot}$). The *IRAS* LRS spectrum between 9-15 μm shows a "broad" feature with a weak FWHM of 4-5 μm, and is attributed to possibly aluminum oxides (Little-Marenin & Little 1990). This lack of definitive dust also supports the case for S Lac having little or no mass loss with respect to dust components. While SiO, H_2O and OH masers are thought to form 2, 10 and 1000 $R_{\star}$ away, respectively (Little-Marenin & Little 1990), no SiO or OH masers have been detected for S Lac (Jewell et al. 1991; Dickinson et al. 1986; Spencer et al. 1981; Dickinson,

1976). H_2O masers have not been detected either. The lack of maser activity around S Lac suggests a mass loss rate $\leq$ 5 x 10^{-8} $M_\odot$/yr (Benson & Little-Marenin, 1996). Thus, even if the supposition by Dyck et al. (1992) - that effects due to dust are not significant in the K band - is not valid, the mass-loss rates of RZ Peg and S Lac are still low enough not to warrant dust as a consideration for the effects seen in the narrowband angular diameters of each star.

4.3. Linear Radii and Pulsation Mechanism

Converting the 2.2 μm angular sizes to linear radii strictly depends upon distance determinations. Parallax measurements for S Lac from the *Hipparcos* catalog (Perryman et al. 1997) are of the same order as its angular size, and due to pulsation, that size is changing with time. This makes the parallax problematic to measure with any sense of accuracy and may account for the large uncertainty in the measurement (1.50 $\pm$ 1.65 mas). Determinations of distance will have to rely upon absolute magnitudes for S Lac. Whitelock, Marang & Feast (2000) quote a distance of 960 pc. Yet, the photometry from Gezari et al. (1999) along with the period-luminosity relation by Whitelock & Feast (2000) puts the star about 250 pc farther out. The distance determination for RZ Peg suffers similar discrepancies. The uncertainty in the *Hipparcos* parallax is of the same size as in S Lac, with a quoted measurement of 3.54 $\pm$ 1.34 mas. However, this parallax is of the same size as the angular diameter of RZ Peg, and given the large change in visual magnitude of both RZ Peg and S Lac, the parallax measurements of *Hipparcos* are not considered herein. As in the case of S Lac, methods used to determine distance of RZ Peg based on absolute magnitudes are utilized. Distances from other sources in the literature were included to produce a mean distance for both S Lac and RZ Peg (Table 4), and the value of the scatter in corresponding means (25 - 30%) unfortunately represents the fundamental problem in

converting angular diameters to linear radii.

This large discrepancy in distance determination also makes the mode of pulsation difficult to establish in S Lac. Using the period-mass-radius (PMR) relation of Ostlie & Cox (1986), S Lac can span the region of being a high-mass (1.4 $M_{\odot}$) star pulsating in fundamental mode to a solar-mass (0.8 - 1.0 $M_{\odot}$) star pulsating in the first overtone mode. A similar result is found when using the period-radius relation by van Leeuwen et al. (1997), as S Lac is found to be either a high mass ($\simeq$ 2 $M_{\odot}$) fundamental pulsator, or a low-mass ($\simeq$ 0.8 $M_{\odot}$) first-overtone pulsator. Clearly, this is due to the spread in values for the distance determination used herein. And, while the results of van Leeuwen et al. (1997) suggest that Miras with periods shorter than 400 d tend to pulsate in an overtone, both sources for pulsation mode above do not account for shock phenomena as evidenced by excitation lines in the spectra of Mira variables. Models which do account for these effects favor almost exclusively fundamental mode pulsation (Bessell, Scholz & Wood 1996).

The pulsation mode of RZ Peg is equally difficult to determine definitively, due also to the large discrepancies in distance determination. When the parameters for RZ Peg are applied to the PMR realtion of Ostlie & Cox (1986), the mass ranges similar to that found for S Lac result. Again, RZ Peg could be a solar-mass overtone pulsator, or a high mass fundamental pulsator. Without better distance determinations, the mystery of pulsation mode for both S Lac and RZ Peg cannot be definitively resolved.

4.4. Molecular photospheres

As to the bandedge apparent angular sizes in both Miras S Lac and RZ Peg, they should not be taken as direct proxies for linear radii when used in conjuction with a distance determination. We interpret the bandedge apparent diameters of S Lac first. Effects due to

opacity of molecular species which enshroud S Lac are superimposed over the continuum flux, and result in a larger apparent angular size in the bandedges. However, information as to the *nature* of these molecular species can be explored. If one considers a model in which a molecular envelope surrounds the stellar photopsphere, as in the case of Bessell, Scholz & Wood (1996) and Scholz (2001), the nature of the angular sizes in the bandedges becomes clearer.

Without high-resolution spectroscopic data, it is impossible to determine the location and velocity of the H_2O opacity source about S Lac. The most dominant chemical component contributing to the K-band opacity in oxygen-rich Miras is H_2O, as seen in some representative flux spectra (Fig. 4). Using the spectra of Lançon & Wood (2000), it can be easily seen that H_2O molecular opacity has significant effects on both edges of the K band. The PTI channels, indicated by vertical lines in Fig. 4, are affected by these water absorptions. Hinkle & Barnes (1979) have shown, with high-resolution spectroscopy, that the majority of the H_2O in the atmosphere of an oxygen-rich Mira variable (R Leo) can exist not only in a circumstellar "warm" region ($T \simeq 1000$ K) about the star, but also at the atmospheric boundary layers at $T_{eff} \simeq 2500$ K. Due to the relatively lower effective temperatures of Mira variables, water of greater abundance can exist about the parent star than exists about the hotter supergiant M-type stars (Tsuji, 2000). These effects for Miras can be seen in Fig. 4 for the two oxygen-rich Miras UZ Her and RZ Car. As a result of the Miras lower effective temperatures, water would then be in abundance much closer to the stellar photosphere than in their supergiant counterparts.

Examining the best-fit cycloids of the 2.0 and 2.2 μm narrowband diameters in S Lac, no phase lag exists between these two wavelength-dependent diameters. This lack of a phase lag suggests the source of H_2O opacity is either truly at the stellar photosphere, or lies some distance away and the nature of the angular size changes in the 2.0 μm channel

lend themselves to radiative effects from the continuum. Water cannot form at a stellar photosphere of 3000 - 3500 K, and thus the first supposition is rejected. If the second supposition is valid, then the region between the stellar photosphere and the inner radius of the molecular region must be optically thin with respect to the K band. Additionally, velocity variations in the T $\simeq$ 1000 K component of R Leo found by Hinkle & Barnes (1979) are similar to that of the photosphere, traced by hot CO and OH (Hinkle, 1978). This latter evidence in the oxygen-rich R Leo supports the supposition that the source of the H_2O opacity exists some distance away from the stellar photosphere of S Lac.

As one moves radially outward into the molecular region above the oxygen-rich photosphere, temperatures fall and, as a result, the opacity of H_20 rises. If one assumes a radial temperature distribution appropriate for a gray atmosphere (Reid & Menten 1997) such that

$$T^4(r) = T^4_{R_\star}\left(1 - \sqrt{1 - \frac{R^2_\star}{r^2}}\right) \tag{3}$$

then for a star with a blackbody temperature of T_{BB} = 3200 K, a warm molecular region of T = 2500 K would exist at a distance 1.3 $R_\star$. If the molecular region were dense enough, mechanical lifting of this region by a shock wave would occur in addition to radiative lifting. If one examines the 2.4 μm angular diameters of S Lac, a phase lag of 0.14 exists between these diameters and the 2.2 μm diameters. This phase lag corresponds to $\simeq$ 35 d in S Lac, the time that it would take for a shock wave propagating outward from the stellar photosphere at 20 km/s to reach a distance of 1.3 $R_\star$. This shockwave would lift the molecular region at a time after radiative effects change the size of the continuum layer. Given that water is the dominant source of opacity in the K band for oxygen-rich Miras, the 2.4 μm channel is affected by the broad 2.7 μm absorption due to H_2O. We assert that the phase lag between the 2.2 μm and the 2.4 μm cycloids is attributed to a region

of hot molecular H_2O very close to the stellar photosphere. This view is supported by the models of Bessell, Scholz & Wood (1996) and Hofmann, Scholz & Wood (1998), although their models utilize a cooler molecular region of T = 1500 K and a non-gray temperature decrease with distance from the star (more approriate for M-type Miras). At this lower temperature, the molecular region would exist at $\simeq 3$ $R_\star$ in accordance with Eq. (2). With respect to monochromatic radii and the models of Bessell et al. (1989), the narrowband UD diameters of S Lac are better represented by the 3500 K $\geq T_{eff} \geq$ 2900 K models (X350) than by the cooler 3000 K $\geq T_{eff} \geq$ 2300 K models (X300). Again, this implies that S Lac should be hotter than its derived T_{eff}.

Explicit models with respect to visibilty measurements for carbon-rich Miras do not exist in the literature, thus no direct comparison of the empirical data on RZ Peg can be attempted. The narrowband diameters of RZ Peg all change in size in phase with each other, and the phase lag from visual maximum is the same as that seen in radial velocity measurements of Udry et al. (1998), which measured bulk motions of the stellar photosphere of RZ Peg. Given the lack of a phase lag between the continuum diameter cycloid and the bandedge cycloids for RZ Peg, the existence of a molecular region dense enough to be mechanically lifted by a shockwave is ruled out. Thus, we attribute the lack of phase lags between the continuum diameter and the bandedge diameters to radiative processes, such that the sources of opacity effecting the 2.4 μm channel for RZ Peg must lie either in the stellar photosphere or in an optically thin region some distance form the star. As to the possible constituents of this molecular region, C_2 is ruled out due to its relatively weak absortion characteristics within the K band (Loidl, Lançon & Jorgensen, 2001) as seen in the attempt to model empirical spectra of the carbon star Y Hya. They also note that effects due to CO become stronger as the star becomes more extended (i.e. log(g) becomes smaller, as in the case of Mira variables), whereas C_2 and CN behave in the opposite sense. In the Mira S Cep, Hinkle & Barnbaum (1996) found very strong absorption lines in

the spectra of this rather naked carbon-Mira, and whose radial velocities were attributed to bulk motions in the stellar atmosphere. This implies the source of CN lies at or just above the stellar photosphere of S Cep, as well as other carbon stars (Barnbaum & Hinkle, 1995). In the carbon Mira V Crb, a significant source of opacity at 2.5 μm was found and attributed to HCN and C_2H_2 (Goebel et al. 1981), with these two molecules thought to be formed just beyond the stellar photosphere and carried out by stellar winds (Bieging, Shaked & Gensheimer 2000).

Given that CN is a moderate source of opacity in carbon stars, we cannot definitively rule this molecule out in the molecular region about RZ Peg, and more probably exists in the region just at the stellar photosphere as in the case for S Cep above. The CN would have effect of contaminating the continuum size of RZ Peg, though most certainly to a much lesser degree than H_2O in the case of oxygen-rich Miras. Our derived T_{eff} is consistent with the models of Lobel, Doyle & Bagnulo (1999) for R For, a carbon Mira with an optically thin dust shell with a density structure of the outer envelope following a r^{-2} gradient by radiative pressure on dust and whose T_{eff} = 3200 K. Given the large departure in angular size of the 2.4 μm diameters in RZ Peg (Fig. 1), the most significant sources of opacity about RZ Peg are CO, HCN and C_2H_2, with the $\Delta\nu$=2 transitions of CO known to have blended photospheric and circumstellar contributions (Hinkle, Hall & Ridgway 1982; Tsuji 1988).

4.5. Atmospheric Extension

It is well-known that the stellar atmospheres of Mira variables are much more extended than their non-Mira giant counterparts, owing to the existence of a molecular photosphere (T 1000 - 2000 K) spatially detached from the continuum photosphere. As previously discussed, models which include atmospheric extension attempt to explain opacity effects

as a function of pulsation phase (Bessell et al. 1989; Bessel, Scholz & Wood 1996; Hofmann, Scholz & Wood 1998). It is postulated that Miras with an appreciable molecular photosphere would appear more atmospherically extended at maximum than at minimum light (Yamamura, de Jong & Cami 1999).

By dividing out the effects due to continuum pulsation in both RZ Peg and S Lac, and displaying the results as a function of pulsation phase, the angular size changes of the bandedge data may be explored (Fig. 3). In the case of RZ Peg, the 2.4 μm size changes (relative to the continuum, and hence represent effects *in addition to* the continuum size changes) are more extended near phase 0.9, yet this maximum extension lags behind the maximum continuum size by 0.35 in phase. Udry et al. (1998) measured line-doubling in radial velocity measurements of RZ Peg between phases 0.0 – 0.2, so if a shock emerged from the stellar photosphere near phase 0.9, its effects would be seen just after maximum visual light in RZ Peg. We assert that the shock wave emerging from deep inside the stellar photosphere lifted the stellar photosphere and its atmospheric sources of opacity (CO, HCN, C_2H_2) faster than the effects due to stellar pulsation seen in the continuum size, and hence the phase lag between maximum continuum size and maximum atmospheric extension. Data on RZ Peg taken on three consecutive nights in 1999 (near phase 0.1), show short term size changes in the 2.2 and 2.4 μm channels at the 5 – 6 σ level. These size changes over the interim 48 hours would require expansion velocities between 40 – 50 km/s, while size changes in the 2.0 μm data would require 5 – 10 km/s. Thus, the data are consistent with a region of optically thicker CO/CN) existing above the stellar photosphere, and was lifted mechanically by a shockwave for a short time before the shockwave passed to a optically thinner region. The idea of CO existing at the stellar photosphere and in a region just above is supported by line-broadening of near-infrared CO lines by Hinkle & Barnes (1979). Additionally, in the 2.0 μm channel, the angular size changes tend to change at a rate comparable to those in the 2.2 μm channel. This suggests that CN/HCN/C_2H_2 lie

relatively close to the stellar photosphere, while CO is more spatially extended.

Maximum atmospheric extension is also seen in S Lac for both bandedges, with the 2.0 and 2.4 μm relative sizes peaking near phase 0.9. Given that both the bandedge relative sizes are most extended at the same time, as well as maximum continuum size occuring 0.1 phase later, further supports the source of H_2O opacity occurs some distance beyond the stellar photosphere in S Lac. Most models in the literature also place CO in the same region as the H_2O in oxygen-rich Miras, and CO may also be contributing to the atmospheric extension of S Lac at 2.4 μm (Hinkle & Barnes, 1979). However, as H_2O and CO (and possibly HCN) effect the 2.4 μm channel, it is impossible to draw any conclusions as to where these molecular species exist spatially about S Lac in the PTI dataset.

4.6. Wideband vs. Narrowband diameters

Lastly, we briefly comment on systematic differences in the dataset between the narrowband diameters and the synthetic wideband diameters of both RZ Peg and S Lac. There is evidence that the wideband diameters overestimate the size of the 2.2 μm diameters as a function of phase. For data between the phase interval 0.75 - 0.24, the diameters overestimate the narrowband diameters by 2.7 $\pm$ 0.8 %. For the phase interval 0.25 - 0.74, this value drops to 1.3 $\pm$ 0.5 %. While only three data points exist in the dataset for RZ Peg near visual minimum , the interval near visual maximum yields a wideband overestimation of 1.7 $\pm$ 0.9 %. The spectral shapes seen in Fig. 1, with S Lac possessing two bandedge diameters greater than the continuum and RZ Peg only one, may account for the difference between the two stars at the same phase interval. While these effects are small, the suggestion is that opacity sources in the wings of the K band can overestimate wideband visibility measurements systematically, but is only weakly supported as a function of pulsation phase in S Lac.

5. Conclusions

Using the technique of long-baseline narrowband interferometry, we have systematically observed the carbon-rich Mira RZ Peg and the oxygen-rich Mira S Lac over multiple phase epochs. For S Lac, a mean T_{eff} = 2600 K is derived, with peak-to-peak temperature variations of 250 K deduced from the best-fit continuum cycloid. The nature of the depth of the spectral UD feature for S Lac (15-25 %) is attributed to H_2O as the dominant source of opacity, which is supported by current models of oxygen-rich Miras. The oxygen-rich non-Mira giant displays this feature, but to a much less degree than its Mira counterpart ($\simeq$ 1 %). A phase lag of 0.14 between the continuum and 2.4 μm sizes in S Lac is consistent with a dense molecular region of H_2O (and CO) at 1.3 $R_\odot$ being mechanically lifted by an emerging shockwave. Maximum visual brightness corresponds to minimum continuum size in S Lac, with the atmosphere being at its most extended near the same time.

For RZ Peg, a mean T_{eff} = 2700 K is derived, with peak-to-peak temperature variations of 270 K deduced from the best-fit continuum cycloid. Both RZ Peg and HIP 92194 show a positive slope across the K band with respect to UD angular size, but with the carbon-rich Mira RZ Peg clearly having a slope 2.5 times larger than the non-Mira carbon star. RZ Peg is a relatively naked star, showing little obscuration due to dense opacity sources as evidenced by the small departure from its blackbody temperature. The nature of the angular size changes in the narrowband data suggest CN, HCN and C_2H_2 occur at the stellar photosphere, while CO exists at and/or above the photosphere. Weak evidence suggests that a possible optically thicker region of CO/CN exists just beyond the stellar photosphere, indicated by an increase in angular size over a three-night period which is attributed to a shockwave partially lifting this region mechanically.

The observations of RZ Peg and S Lac are part of a long-term monitoring program of Mira variables at PTI begun in early 1999. At present, the PTI Mira program is tracking

over 70 stars in near-infrared bands, covering a range of chemical subtypes. The program's goals are to observe changes in apparent angular size with respect to pulsation phase and correlate this with chemical abundance, pulsation mode, spatial geometry, and strength of acoustics shocks as evidence of pulsation mode in an attempt to identify overall trends. This is the first in a series of papers on this rather large and varied dataset at PTI.

This work was performed at the Jet Propulsion Laboratory, California Institute of Technology, under contract from the National Aeronautics and Space Administration. Data were obtained at the Palomar Observatory using the NASA Palomar Tested Interferometer, which is supported by NASA contracts to JPL. Science operations with PTI are possible through the efforts of the PTI Collaboration (http://huey.jpl.nasa.gov/palomar/ptimembers.html). The authors wish to gratefully acknowledge Kevin Rykoski and Jean Mueller of Palomar Observatory for their efforts in obtaining the data. This work utilized the AFOEV and SIMBAD databases, operated at CDS, Strasbourg, France.

REFERENCES

Aoki, W., Tsuji, T. & Ohnaka, K., 1998, A+A, 340, 222

Baldwin, et al. 1994, SPIE, 2200, 112

Baranne, A., Mayor, M. & Poncet, J.L. 1979, Vistas Astron., 23, 279

Barnbaum, C. & Hinkle, K.H., 1995, AJ, 110, 805

Beach, T.E., Willson, L.A. & Bowen, G.H. 1988, ApJ, 329, 241

Bedding, T.R., Robertson, J.G. & Manson, R.G. 1994, A+A, 290, 340

Bergeat, J., Knapik, A. & Rutily, B. 2001, A+A, 369, 178

Benson, P.J. & Little-Marenin, I.R., 1996, ApJS, 106, 579

Bessell, M.S., Brett, J.M., Scholz, M. & Wood, P.R. 1989, A+A, 213, 209

Bessell, M.S., Scholz, M. & Wood, P.R. 1996, A+A, 307, 481

Bieging, J.H., Shaked, S. & Gensheimer, P.D. 2000, ApJ, 543, 897

Boden, A.F., Colavita, M. M., van Belle, G.T. & Shao, M. 1998, Proc. SPIE, 3350, 872.

Boden, A.F. et al. 1998, ApJ, 504, L39

Bowen, G.H. & Willson, L.A., 1991, ApJ, 375, L53

Burleigh, M.R., Barstow, M.A. & Fleming, T.A., 1997, MNRAS, 287, 381

Burns, D. et al. 1998, MNRAS, 297, 462

Chiang, E.I. et al. 2001, ApJ, 547, 1077

Colavita, M.M. et al. 1999, ApJ, 510, 505

Colavita, M.M. 1999, PASP, 111, 111

Creech-Eakman, M.J. & Thompson, R.R., *Pulsation Modes of Mira Variables investigated using NIR Interferometry,* August 2001, to appear in *Twelfth Cambridge Workshop on Cool Stars, Stellar Systems and the Sun,* ASP Conference Proceedings

Dickinson, D.F. 1976, ApJS, 30, 259

Dickinson, D.F., Turner, B.E., Jewell, P.R. & Benson, P.J. 1986, AJ, 92, 627

Dominy, J.F., Wallerstein, G. & Suntzeff, N.B. 1986, AJ, 300, 325

Dumm, T. & Schild, H. 1998, New Astron., 3, 137

Dyck, H.M., Benson, J.A., Ridgway, S.T. & Dixon, D.J. 1992, AJ, 104, 1982

Gezari, D.Y., Pitts, P.S. & Schmitz, M. 1999, "Catalog of Infrared Observations", 5th Edition. (Available at CDS, Strasbourg, France)

Goebel, J.H., Bregman, J.D., Whitteborn, F.C., Taylor, B.J. & Wilner, S.P., 1981, ApJ, 246, 455

Groenewegen, M.A.T., Whitelock, P.A., Smith, C.H. & Kerschbaum, F. 1998, MNRAS, 293, 18

Hale, D.D. et al. 2000, ApJ, 537, 998

Hinkle, K.H. 1978, ApJ, 220, 210

Hinkle, K.H. & Barnes, T.G. 1979. ApJ, 227, 923

Hinkle, K.H., Hall, D.N.B. & Ridgway, S.T. 1982, 252, 697

Hinkle, K.H. & Barnbaum, C. 1996, AJ, 111, 913

Hofmann, K.-H., Scholz, M. & Wood, P.R. 1998, A+A, 339, 846

Jacob, A.P., Bedding, T.R., Robertson, J.G. & Scholz, M. 2000, MNRAS, 312, 733

Jewell, P.R., Snyder, L.E., Walmsley, C.M., Wilson, T.L. & Gensheimer, P.D. 1991, A+A, 242, 211

Jura, M. 1986, ApJ, 303, 327

Kerschbaum, F., Lazaro, C. & Habison, P. 1996, A+AS, 118, 397

Kholopov, P.N. et al. 1998, "General Catalog of Variable Stars", 4th ed.

Knapik, A., Bergeat, J. & Rutily, B. 1999, A+A, 344, 263

Lançon, A. & Rocca-Volmerange, B. 1992, A+AS, 96, 593

Lançon, A. & Wood, P.R. 2000, A+AS, 146, 217

Le Bertre, T. & Winters, J.M. 1998, A+A, 334, 173

Lewis, B.M. 1989, AJ, 98, 1814

Little-Marenin, I.R. & Little, S.J. 1990, AJ, 99, 1173

Lobel, A., Doyle, J.G. & Bagnulo, S. 1999, A+A, 343, 466

Loidl, R., Lançon, A., & Jorgensen, U.G. 2001, A+A, 371, 1065

Lu, P.K. et al. 1987, AJ, 94, 1318

Morel, M. & Magnenat, P. 1978, A+AS, 34, 477

Mennessier, M.O., Boughaleb, H. & Mattei, J.A. 1997, A+AS, 124, 143

Noguchi, K. & Akiba, M. 1986, PASJ, 38, 811

Ostlie, D.A. & Cox, A.N. 1986, ApJ, 311, 864

Perrin, G. et al. 1999, A+A, 345, 221

Perryman, M.A.C., et al. 1997, A+A, 323, L49

Quirrenbach, A. 2001, ARA+A, 39, 353

Reid, M.J. & Menten, K.M. 1997, ApJ, 476, 327

Scholz, M. 2001, MNRAS, 321, 347

Spencer, J.H., et al. 1981, AJ, 86, 392

Spinrad, H. & Wing, R.F. 1969, ARA+A, 7, 249

Thompson, R.R., Creech-Eakman, M.J. & Akeson, R.L. 2001, submitted to ApJ

Thompson, R.R. 2002, Ph.D thesis

Tsuji, T. 1988, A+A, 197, 185

Tsuji, T. 2000, ApJ, 538, 801

Tuthill, P.G., Monnier, J.D. & Danchi, W.G. 1999, ASP Conference Series, 194, S.C. Unwin & R.V. Stachmick, eds.

Tuthill, P.G., Danchi, W.G., Hale, D.S., Monnier, J.D. & Townes, C.H. 2000, ApJ, 534, 937

Udry, S., Jorissen, A., Mayor, M. & van Eck, S. 1998, A+AS, 131, 25

van Belle, G.T., Dyck, H.M., Benson, J.A. & Lacasse, M.G. 1996, AJ, 112, 2147

van Belle, G.T. Dyck, H.M., Thompson, R.R., Benson, J.A. & Kannapan, S.J. 1997, AJ, 114, 2150

van Belle, G.T. & Thompson, R.R. 1999, BAAS, 195, 45.01

van Belle, G.T. et al. 2002, in preparation

van Leeuwen, F., Feast, M.W., Whitelock, P.A. & Yudin, B. 1997, MNRAS, 287, 955

Wallerstein, G. & Knapp, G.R. 1998, ARA+A, 36, 369

Whitelock, P.A. 1986, MNRAS, 219, 525

Whitelock, P. & Feast, M. 2000, MNRAS, 319, 759

Whitelock, P., Marang, F. & Feast, M. 2000, MNRAS, 319, 728

Wing, R.F. & Spinrad, H. 1970, ApJ, 159, 973

Wyatt, S.P. & Cahn, J.H. 1983. ApJ, 275, 225

Yamamura, I., de Jung, T. & Cami, J. 1999, A+A, 348, L55

Yamashita, Y. 1972, Ann. Tokyo Obs., 13, 167

Young, J.S. et al. 2000, MNRAS, 318, 381

This manuscript was prepared with the AAS LaTeX macros v5.0.

Table 1. Calibration stars for both RZ Peg and S Lac.

Name	Catalog ID	Sp Type	m_V (mag)	m_K (mag)	UD estimated diameter (mas)
HR 8320	HD 207088	G8 III	6.5	4.3	0.73 ±0.10
29 Peg	HD 210459	F5 III	4.3	3.1	0.88 ±0.13

Table 2. Fit Parameters [a]of the Cycloids Y=a x cos(2π(ϕ+b))+c given in Fig. 2.

Y	a	b	c	χ^2_μ	P
RZ Peg 2.0 μm diameter	0.34 ± 0.03	-0.28 ± 0.03	2.64 ± 0.02	14.2	30
2.2 μm diameter	0.28 ± 0.02	-0.28 ± 0.02	2.83 ± 0.02	14.6	22
2.4 μm diameter	0.27 ± 0.02	-0.23 ± 0.03	3.35 ± 0.02	13.8	18
S Lac 2.0 μm diameter	0.19 ± 0.02	0.53 ± 0.03	3.19 ± 0.02	14.2	13
2.2 μm diameter	0.28 ± 0.02	0.48 ± 0.02	2.89 ± 0.02	9.5	21
2.4 μm diameter	0.19 ± 0.02	0.34 ± 0.02	3.48 ± 0.03	12.1	12

[a]Y = angular diameter (mas), a = amplitude, ϕ = pulsation phase, b = phase offset, c = linear offset (i.e. mean value of cycloid), $\chi^2_\mu = \chi^2$ of fit per degree of freedom, P = maximum percent change in size relative to minimum size.

Table 3. Source parameters for the Miras.

Name / ID	RZ Peg	HD 209890	S Lac	HD 213191
Spectral Type	C6e,II		M4-M8e III	
Visual (mag)	8.4-12.8	AFOEV data	8.2-13.1	AFOEV data
K-band (mag)	2.9	Gezari et al. (1999)	2.5	Gezari et al. (1999)
Period (d)	422.4	this work, epoch JD 2451373	240.6	this work, epoch JD 2451249
Visual curve asymmetry	0.44	Mennessier et al. (1997)	0.45	Mennessier et al. (1997)
Mean continuum angular diameter [a](mas)	2.83±0.02	this work	2.89±0.02	this work
Bolometric flux (erg/cm^2/s)	14.3±0.8 x 10^{-8}	fit to available photometry	12.80±0.9 x 10^{-8}	fit to available photometry[c]
Effective temperature (K)	2706 ± 36	T_{eff}=2341 $(F_{bol}/\theta^2)^{1/4}$	2605±47	T_{eff}=2341 $(F_{bol}/\theta^2)^{1/4}$
Mean linear radius ($R_\odot$)	377 ± 111	this work	292 ±73	this work

[a]Represents the mean of the cycloid in Table 2 for the 2.2 μm diameter.

[b]Using photometric data longward of 1 μm from Gezari et al. (1999)

[c]Using photometric data longward of 1 μm from Noguchi & Akiba (1986) and Morel & Magnenat (1978)

Table 4. Distance determination for RZ Peg and S Lac.

RZ Peg Distance (pc)	Reference	S Lac Distance (pc)	Reference
1700	Whitelock & Feast (2000)	960	Whitelock & Feast (2000)
1230	Whitelock, Marang & Feast (2000); Gezari et al. (1999)[a]	1225	Whitelock,Marang & Feast (2000); Gezari et al. (1999)[a]
800	Dominy et al. (1986)	928	van Leeuwen et al. (1997)
1230	Groenewegen et al. (1998)	650	Wyatt & Cahn (1983)
1240 ± 368	MEAN	941 ± 235	MEAN

[a]Using the period-luminosity relation of Whitelock, Marang & Feast (2000), for respective chemical classes ("Miras only"), with apparent K magnitudes from Gezari et al. (1999).

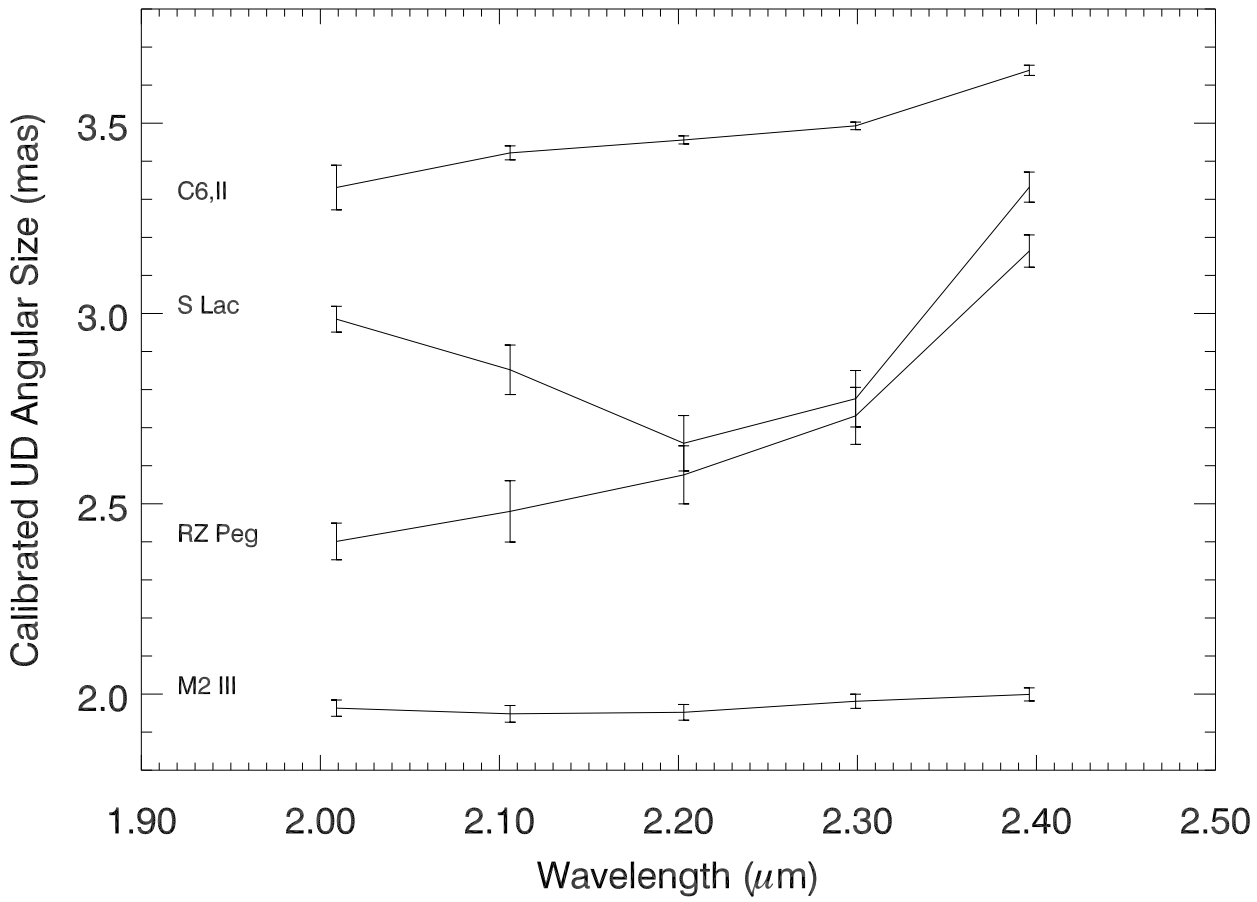

Fig. 1.— Calibrated UD spectral angular sizes for Miras and non-Miras. Both Mira stars exhibit greater degrees of size departures from their continuum than do the non-Mira chemical counterparts. These representative data were taken on the same night (JD 2451715). Top to Bottom: HIP 92194 (C6,II), S Lac (M4-M8e), RZ Peg (C5-6e,I), HD 193347 (M2 III)

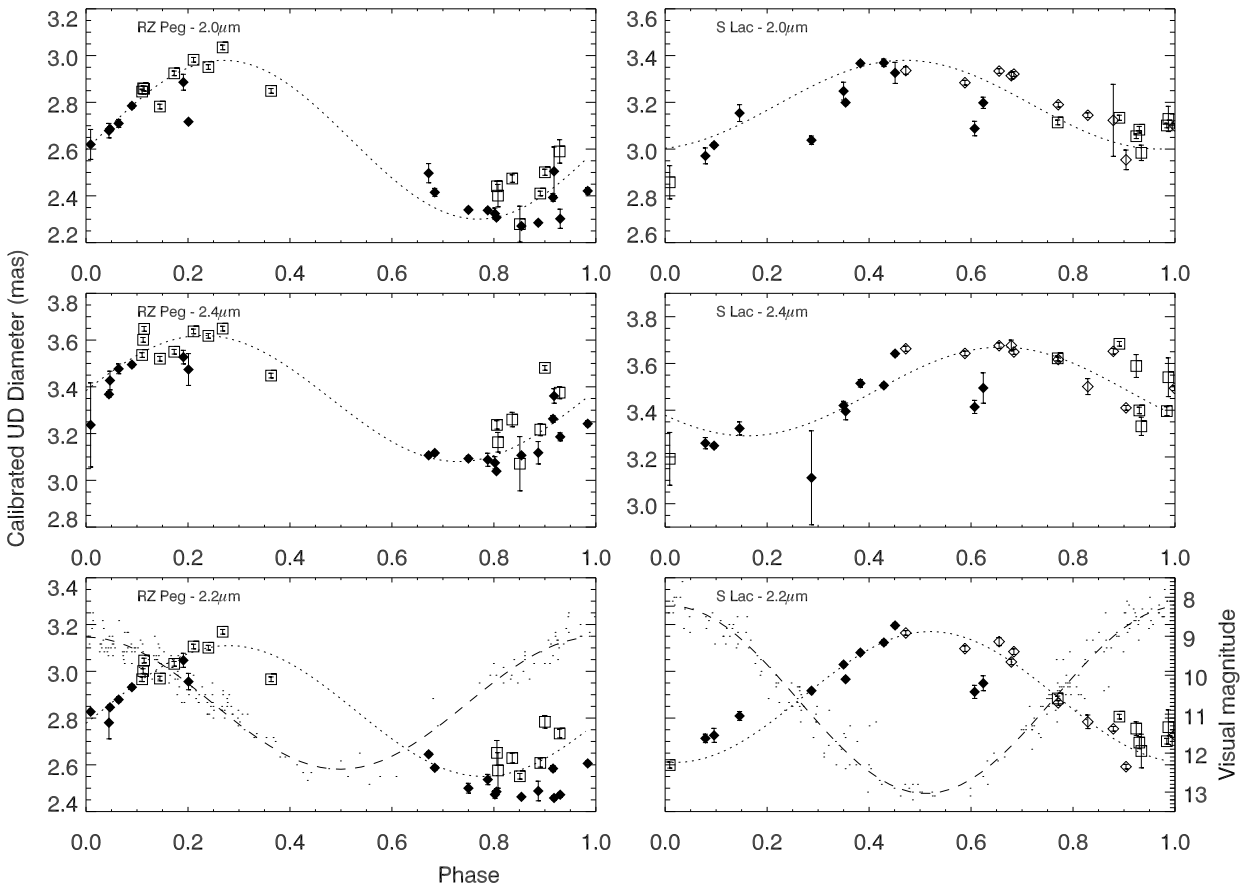

Fig. 2.— Calibrated UD spectral angular size vs. phase for RZ Peg and S Lac. The top four plots depict the red and blue bandedge sizes, the bottom two plots depict the continuum sizes overlaid with the visual magnitude data, as indicated by the dashed curves. The curves represent the best sinusoid fit to the angular size data (see Table 2). Phase offsets with respect to visual cycles are described in the text. (For RZ Peg, open symbols depict observations for the first cycle, filled symbols for the second. For S Lac, open symbols depict phases 0.7 - 2.0, filled symbols depict phases 2.0 - 3.8.)

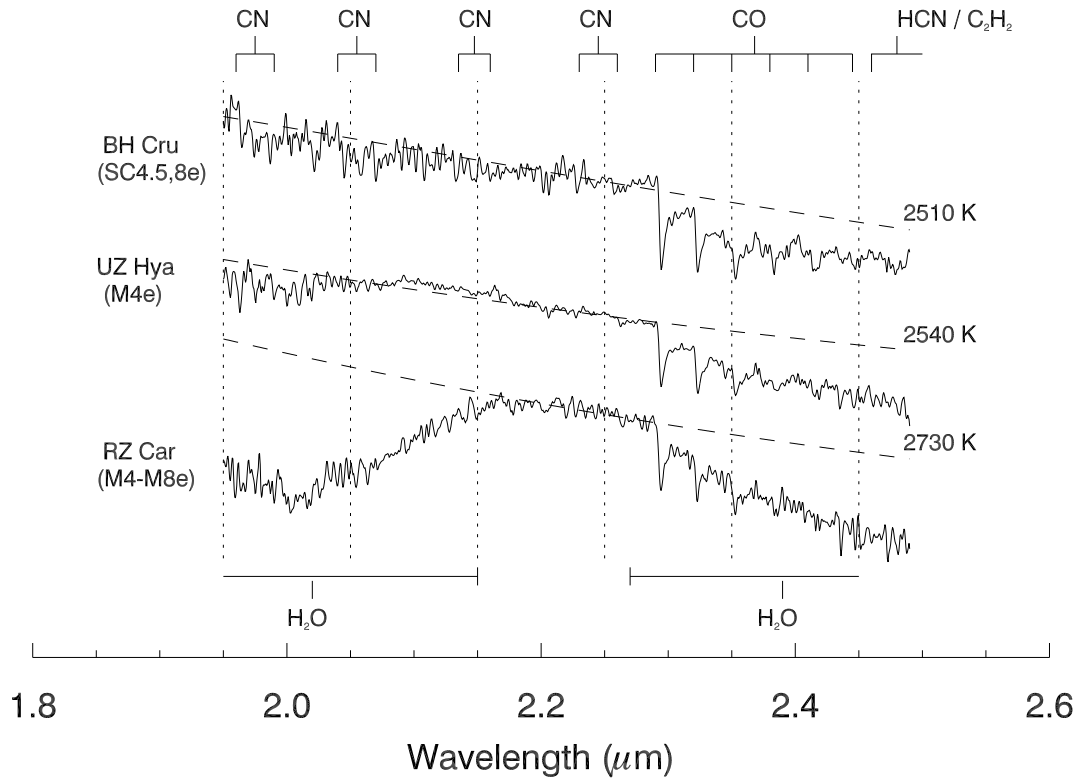

Fig. 3.— K band relative fluxes for a few sample Mira stars, with significant molecular lines indicated. The vertical lines represent the edges of the PTI spectral channels. Color temperatures were fit to H band and K band continuum colors (H band not shown). All three Miras display CO absorption bandheads, while only the two oxygen-rich Miras (UZ Her, RZ Car) display absorption on the blue bandedge. The earlier Mira (M4e) shows this blue absorption to a lesser degree than its later counterpart (M4e-M8e). *(Adapted from Lançon & Wood, 2000.)*

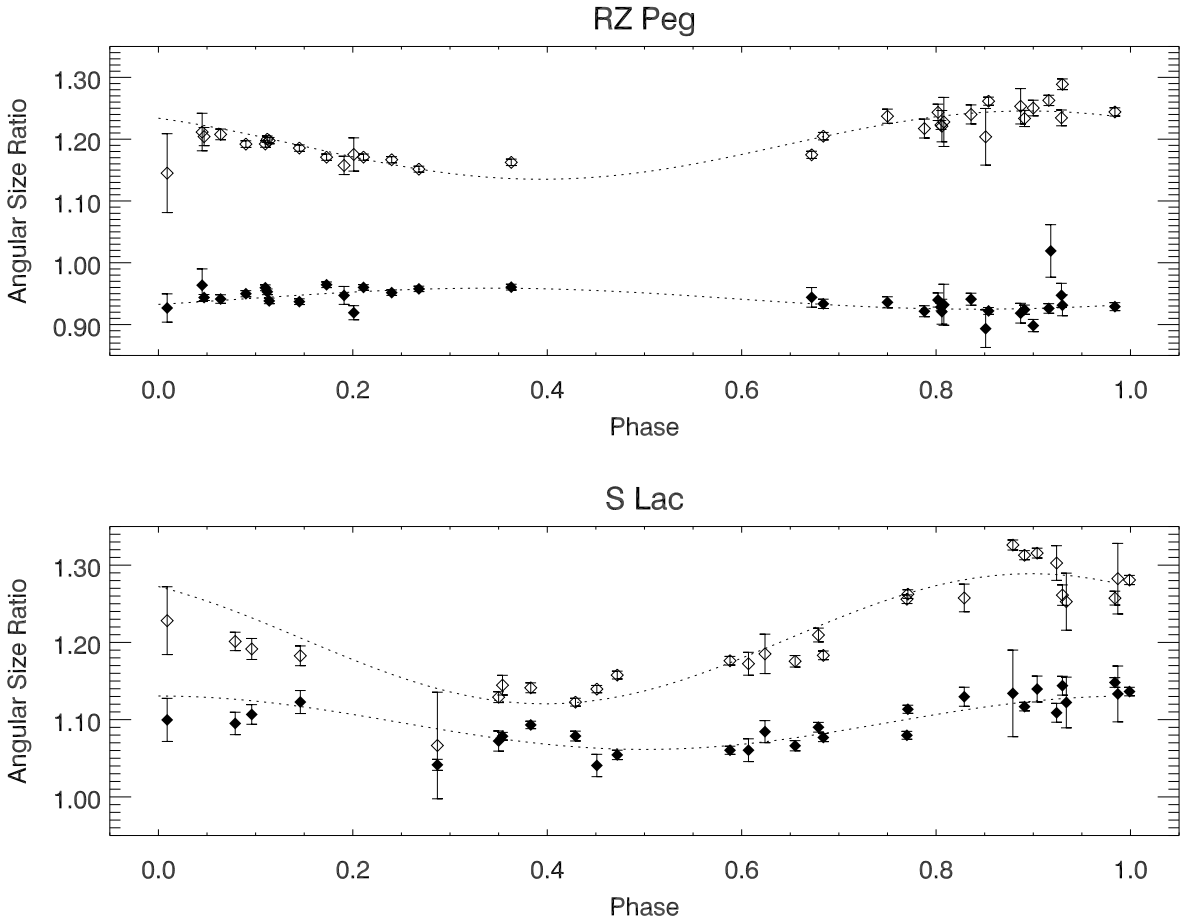

Fig. 4.— Bandedge angular size ratios with respect to the continuum sizes for RZ Peg and S Lac. By dividing out the continuum pulsation sizes, angular size changes beyond continuum pulsation can be seen. In each case, the 2.4 μm sizes change more rapidly than those of their respective continuum. While the 2.0 μm size for the carbon-rich Mira (RZ Peg) changes slightly, the size of the oxygen-rich Mira (S Lac) in the same band has a higher amplitude of cycle. (Open symbols = 2.4 μm, filled symbols = 2.0 μm)